

## Evidence for the contribution of $0f_{5/2}, 1p_{3/2}$ proton excitations in the low-lying states in $^{92,94}\text{Zr}$

H. Mach,<sup>(1)-(3)</sup> E. K. Warburton,<sup>(3),(4)</sup> W. Krips,<sup>(3),(5)</sup> R. L. Gill,<sup>(3)</sup> and M. Moszyński<sup>(2),(3)</sup>

<sup>(1)</sup>*The Studsvik Neutron Research Laboratory, S-61182 Nyköping, Sweden*

<sup>(2)</sup>*Institute for Nuclear Studies, PL 05-400, Świerk-Otwock, Poland*

<sup>(3)</sup>*Brookhaven National Laboratory, Upton, New York 11973*

<sup>(4)</sup>*Universität Heidelberg and the Max-Planck-Institut für Kernphysik, Heidelberg, Federal Republic of Germany*

<sup>(5)</sup>*Institut für Kernphysik, Universität zu Köln, D-5000 Köln 41, Federal Republic of Germany*

(Received 5 March 1990)

Lifetimes of  $T_{1/2}=88(3)$  and  $291(11)$  ps were measured for the  $0_2^+$  states and  $T_{1/2}=102(3)$  and  $500(13)$  ps for the  $4_1^+$  states in  $^{92,94}\text{Zr}$ , respectively, using a recently developed  $\beta$ - $\gamma$ - $\gamma$  fast timing method. The observed  $B(E2)$  values and the recently measured  $g$  factors for the  $2_1^+$  states in  $^{92,94}\text{Zr}$  deviate strongly from properties of a pure  $\nu 1d_{5/2}$  multiplet and even from the  $\pi(1p_{1/2}, 0g_{9/2})\nu(1d_{5/2}, 2s_{1/2})$  shell-model results of Gloeckner. The experimental results are reproduced, however, by spherical shell model calculations with a model space of  $\pi(0f_{5/2}, 1p_{3/2}, 1p_{1/2}, 0g_{9/2})\nu(1d_{5/2}, 2s_{1/2}, 1d_{3/2}, 0g_{7/2})$  and provide compelling evidence for important contributions of  $\pi f_{5/2}, p_{3/2}$  orbits to the low-energy structure of these nuclei.

Many structural similarities between  $^{90}\text{Zr}$  and  $^{96}\text{Zr}$  (see Ref. 1) as well as between  $^{92}\text{Zr}$  and  $^{94}\text{Zr}$  (see Fig. 1) can be understood in simple terms of almost complete subshell closures at  $Z=40$  and  $N=50, 56$ . Nevertheless, for nuclei near  $Z=40$  the  $\pi 1p_{1/2}$  and  $\pi 0g_{9/2}$  orbits are sufficiently close in energy to expect considerable mixing of both orbits in the wave functions of the low-lying levels of Zr and Nb isotopes. Likewise the  $\nu 2s_{1/2}$  and  $\nu 1d_{5/2}$  orbits are close lying so that both neutron orbits should contribute significantly to the low-lying levels of the  $^{90-96}\text{Zr}$  isotopes. Indeed, it was demonstrated by Gloeckner<sup>5</sup> that many properties of the  $N=50-56$  Zr and Nb isotopes can be explained in a simple  $\pi(1p_{1/2}, 0g_{9/2})\nu(1d_{5/2}, 2s_{1/2})$  shell-model space. Among those properties are binding energies and energy spectra, one- and two-particle transfer, and some electromagnetic transition rates. As an example, the calculation reproduces quite well the rising proton occupancy of the  $\pi 1p_{1/2}$  orbit for the Zr isotopes as neutrons are added from  $N=50$  to  $N=56$ . It is of interest that the Gloeckner wave functions for the Zr isotopes are far from a simple closed  $\pi 1p_{1/2}$  subshell coupled to  $(\nu 1d_{5/2})^{N-50}$ —for instance, this component only contributes 56% to the  $^{94}\text{Zr } 0_1^+$  wave function.

In order to ascertain the role of orbits outside the Gloeckner model space, one could consider  $E0$  transitions connecting  $0^+$  states. However,  $E0$  rates are highly dependent on the capricious mixing of the monopole mode into the low-lying states which masks admixtures of the other orbits near the Fermi surface. Magnetic moments and  $E2$  rates are more reliable probes and these are considered here. Indeed, the  $g$  factors measured<sup>6</sup> for the  $2_1^+$  states in  $^{92,94}\text{Zr}$  of  $-0.03(5)$  and  $-0.26(6)$ , respectively, are considerably smaller than the Schmidt value of  $g(\nu d_{5/2})=-0.76$ . They are also considerably smaller than the Gloeckner predictions which we calculate to be  $g=-0.59$  and  $-0.70$  for  $^{92}\text{Zr}$  and  $^{94}\text{Zr}$ , respectively.

Thus, it is likely that these  $g$  factors are sensitive to admixtures of other orbits as suggested by Hass *et al.*<sup>6</sup> Such admixtures were found in a recent shell-model study of  $^{96}\text{Y}$  and  $^{96}\text{Zr}$ .<sup>7</sup> These latter calculations could largely account for the fast first-forbidden  $\beta$ -decay rate for  $0^-$   $^{96}\text{Y} \rightarrow 0^+$   $^{96}\text{Zr}^g$  as well as the small spectroscopic factors for the proton pickup reaction on  $^{96}\text{Zr}$ .

It is the purpose of this article to test the structure of the low-lying levels in  $^{92,94}\text{Zr}$ : experimentally, by measuring the lifetimes of the  $0_2^+$  and  $4_1^+$  levels, and theoretically via spherical shell-model calculations.  $B(E2)$  rates and  $g(2_1^+)$  factors, which show large differences between  $^{92}\text{Zr}$  and  $^{94}\text{Zr}$ , as well as level excitation energies are well reproduced in the calculations, which provide compelling evidence for a more complex level composition with a key role played by vacancies in the  $f_{5/2}-p_{3/2}$  orbits of the proton core.

The lifetimes were measured at the TRISTAN fission product mass separator at Brookhaven National Laboratory using a recently developed  $\beta$ - $\gamma$ - $\gamma$  fast timing method, which is described in Refs. 8–11 and which can measure lifetimes in the subnanosecond range. Briefly, levels in  $^{92}\text{Zr}$  ( $^{94}\text{Zr}$ ) were populated by  $\beta$  decay of  $^{92}\text{Y}$  ( $^{94}\text{Y}$ ) produced from a mass separated source of  $^{92}\text{Rb}$  ( $^{94}\text{Rb}$ ) via a  $\beta$ -decay chain:  $\text{Rb} \rightarrow \text{Sr} \rightarrow \text{Y}$ . Lifetime information is obtained from  $\beta$ - $\gamma$  delayed coincidences in fast timing detectors (a thin NE111A plastic for  $\beta$ -rays and a small  $\text{BaF}_2$  crystal for  $\gamma$  transitions). The  $\Delta E \beta$  detector provides a  $\beta$  response almost independent of the feeding  $\beta$ -ray energy and eliminates the need for a walk determination in this detector. Additional  $\gamma$  coincidences with a Ge detector serve to select a decay branch of interest. The good timing resolution—which ranged from  $\text{FWHM}=155$  ps at  $E_\gamma=380$  keV to 96 ps at  $E_\gamma=1.3$  MeV—allowed the long lifetimes of the  $0_2^+$  and  $4_1^+$  levels to be measured directly from the delayed slope of the

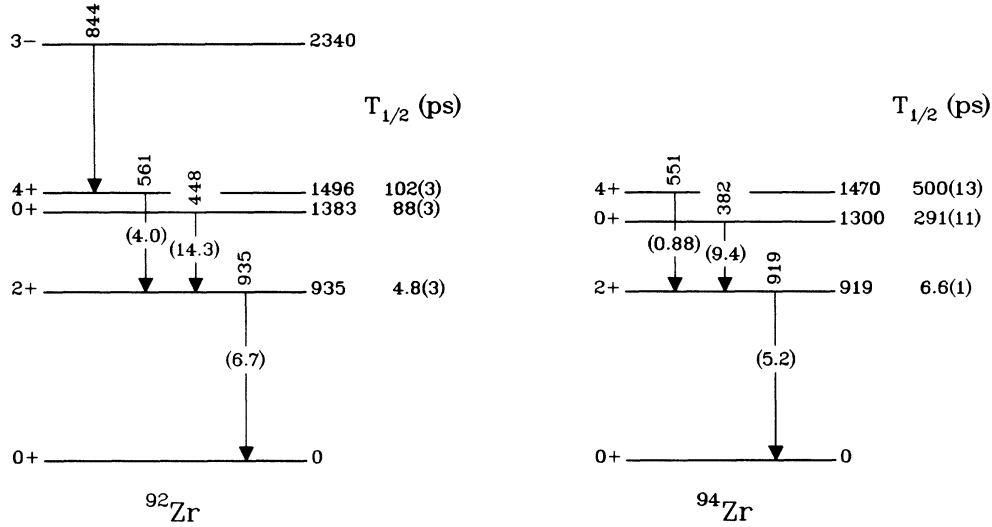


FIG. 1. Partial level schemes (Refs. 2 and 3) for  $^{92,94}\text{Zr}$  indicating a similarity between the structures of these nuclei. Level half-lives which are shown to the right of the energy bar are from this work except for the  $2_1^+$  states for which  $T_{1/2}$  is from Ref. 4. The experimental  $B(E2)$  rates expressed in W.u. are given in parentheses within the transition arrow.

time spectrum (see Fig. 2). The time spectra were deconvoluted only after it was verified by the centroid shift method that no significant delayed component comes from an indirect  $\gamma$  feeding from higher-lying levels. The lifetimes of the  $2_1^+$  levels,  $T_{1/2} \sim 6$  ps, are too short to affect the deconvolution results. For each level, time spectra selected by different gating transitions were deconvoluted and the results verified by the centroid shift analysis. Table I summarizes the experimental results. The present high precision results resolve a previous discrepancy in the lifetimes of the  $0_2^+$  states in favor of the more recent results reported by Julin *et al.*<sup>12</sup>

The  $B(E2)$  values for  $^{92,94}\text{Zr}$  are only weakly collective. The  $B(E2; 2_1^+ \rightarrow 0_1^+)$  values are the lowest in the region;<sup>4</sup> even lower than for the  $N=50$  isotones from  $40 \leq Z \leq 80$ .

In similarity to the  $g$  factors one observes a strong difference between the  $B(E2; 4_1^+ \rightarrow 2_1^+)$  values in  $^{92}\text{Zr}$  and  $^{94}\text{Zr}$  with the  $4_1^+ \rightarrow 2_1^+$   $E2$  rate in  $^{92}\text{Zr}$  four times faster than in  $^{94}\text{Zr}$ . Thus in general, the new lifetime results as well as the  $g$ -factor results suggest significant differences in the structure of the low-lying levels in  $^{92}\text{Zr}$  and  $^{94}\text{Zr}$ . In order to understand these differences we have undertaken shell-model calculations in a significantly expanded model space.

The  $A=90-98$  Zr isotopes have been considered by Gloeckner<sup>5</sup> in a shell-model space composed of the proton  $1p_{1/2}-0g_{9/2}$  orbits and the neutron  $1d_{5/2}-2s_{1/2}$  orbits. The parameters of the interaction were determined by a least-squares fit to experimental binding energies. Considering the severe truncation of this model space, the in-

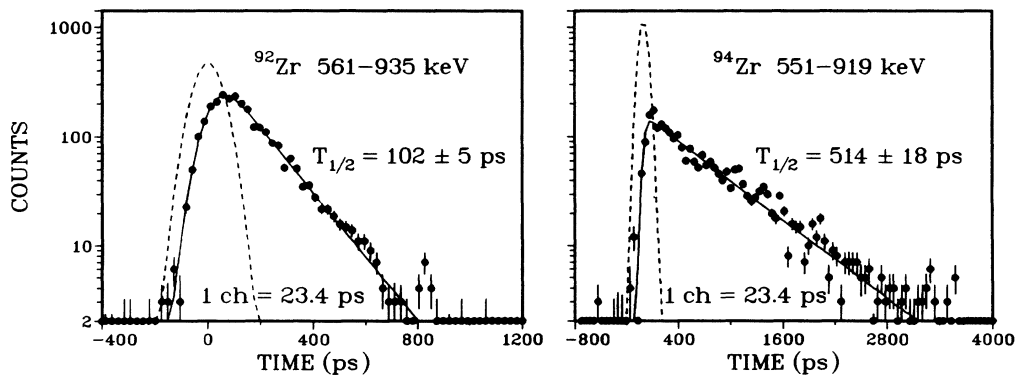


FIG. 2. Left: Delayed time spectrum for the  $4_1^+$  level in  $^{92}\text{Zr}$  obtained with the 561-keV Ge gate and the 935-keV  $\text{BaF}_2$  gate. The  $\chi^2$  fit (solid line) is for  $T_{1/2} = 102$  ps with a prompt component approximated by a Gaussian (broken line). Right: Delayed time spectrum for the  $4_1^+$  level in  $^{94}\text{Zr}$  obtained with the 551-keV Ge gate and the 919-keV  $\text{BaF}_2$  gate; the  $\chi^2$  fit curve is for  $T_{1/2} = 514$  ps.

TABLE I. Summary of experimental lifetimes and transition rates in  $^{92,94}\text{Zr}$ .

Nucleus	$E_x, J^\pi$ (keV)	Gating $\gamma$ -ray <sup>a</sup> (keV)	$T_{1/2}$ this work (ps)	$T_{1/2}$ previous work <sup>b</sup> (ps)	$B(E2)_{\text{exp}}$ (W.u. <sup>c</sup> )
$^{92}\text{Zr}$	935 $2_1^+$			4.8(3)	6.7(5)
	1383 $0_2^+$	935-448	90(5)		
		448-935	<u>86(4)</u>		
			88(3)	85(15)	14.3(5)
	1496 $4_1^+$	935-561	100(5)		
		844-935	98(9)		
844-561		107(7)			
561-935		<u>102(5)</u>			
		102(3)		4.0(1)	
$^{94}\text{Zr}$	919 $2_1^+$			6.6(14)	5.2(11)
	1300 $0_2^+$	919-382	300(15)		
		382-919	<u>281(15)</u>		
			291(11)	280(40)	9.4(4)
	1470 $4_1^+$	919-551	487(17)		
551-919		<u>514(18)</u>			
		500(13)		0.88(2)	

<sup>a</sup>The following convention is used: For the 935-448 time spectrum energy gates were set on the 935-keV peak in the Ge detector and on the 448-keV peak in the BaF<sub>2</sub> spectrum.

<sup>b</sup>References 4 and 12.

<sup>c</sup>The ratio between  $B(E2)$  in  $e^2 \text{fm}^4$  and W.u. is 24.672 and 25.390 for  $^{92}\text{Zr}$  and  $^{94}\text{Zr}$ , respectively.

teraction was extremely successful in describing much of the available experimental data. However, it fails to predict low-lying  $\frac{3}{2}^-$  and  $\frac{5}{2}^-$  levels in the odd Y isotopes and, in the heavier odd Zr isotopes,  $\frac{3}{2}^+$  and  $\frac{7}{2}^+$  levels. Our shell-model interaction takes the Gloeckner interaction as its basis but adds the proton  $0f_{5/2}-1p_{3/2}$  orbits and the neutron  $1d_{3/2}-0g_{7/2}$  orbits. The details of the construction of this interaction were described previously.<sup>7</sup> Since the effect of these additional orbits is perturbative on the Gloeckner (G1) interaction, we do not change the parameters of the G1 interaction. Specifically, the relative  $\pi p_{1/2}-g_{9/2}$  and  $\nu d_{5/2}-s_{1/2}$  single-particle energies (SPE) are kept fixed at the G1 values. The experimental spectra would be better reproduced if the G1 part of the interaction were diminished somewhat in strength as might be expected to result from an expansion of the model space; however, such refinements would not change the basic physics and were not considered. Since we take the additional necessary proton two-body matrix elements from the  $N=50$  interaction of Ji and Wildenthal<sup>13</sup> we shall label our interaction GJW. The SPE for the additional four orbits were determined for the odd Y and Zr isotopes by comparison to proton pickup<sup>14</sup> and neutron stripping<sup>15</sup> data for the  $\pi f_{5/2}-p_{3/2}$  and  $\nu d_{3/2}-g_{7/2}$  orbits. It was found that they were well represented by a linear dependence on  $A$  for  $A=89-97$  and such a smooth dependence was used in the calculations on  $^{92-94}\text{Zr}$ .

The calculations were done using the shell-model program OXBASH.<sup>16</sup> Initial exploratory calculations were done to ascertain the relative importance of the various

partitions contributing to the wave functions in question, a partition being a specific occupancy of the active orbits. It was found that the  $\nu g_{7/2}$  orbit could be ignored with a negligible effect on the results. Restrictions on the available computer disk space dictated the size of the model space for the remaining seven orbits. For  $^{92}\text{Zr}$  the two active neutrons were allowed all possible partitions among the three orbits; while the occupancy of the  $\pi g_{9/2}$  orbit was restricted to at most two protons with no further restriction on the occupancy of the proton orbits. This model space gave a dimension of 1954 for  $J^\pi=4^+$ . For  $^{94}\text{Zr}$ , a first attempt was made with the same proton model space as for  $^{92}\text{Zr}$ , but with the neutron model space constrained to at most two neutrons out of the  $\nu d_{5/2}$  orbit; call this truncation  $T$ . This was found to be too ambitious and 25 of the most energetically favored partitions were chosen from this model space. Various tests—consisting of calculations in which different groups of partitions were sequentially eliminated—indicated that the 25-partition model space was a quite adequate approximation to truncation  $T$ . The  $J$  dimension for the  $4^+$  states was 1523.

The  $B(E2)$  values are calculated with effective charges. For the G1 interaction we use the proton effective charge of  $e_p=0.765e$  adopted by Gloeckner<sup>5</sup> and for  $e_n$  we use a value midway in the range of values reported by Gloeckner for  $^{91-96}\text{Zr}$ ,  $e_n=1.15$ . For the GJW interaction we assumed  $e_p=e_n$  and adjusted this effective charge to reproduce the experimental  $^{92}\text{Zr}$   $4_1^+ \rightarrow 2_1^+$   $B(E2)$  value. For the  $M1$  operator we quench the spin part of the free-nucleon  $M1$  operator by a factor of 0.8

TABLE II. Results of GJW calculations for excitation energies and mean orbit occupancies for the  $^{92}\text{Zr}$  and  $^{94}\text{Zr}$  states of interest in the present study.

$J_k^\pi$	State $E_x$ (keV)	Proton orbit				Neutron orbit		
		$f_{5/2}$	$p_{3/2}$	$p_{1/2}$	$g_{9/2}$	$d_{5/2}$	$s_{1/2}$	$d_{3/2}$
$^{92}\text{Zr}$								
$0_1^+$	0	5.800	3.733	1.134	1.333	1.727	0.215	0.058
$0_2^+$	1711	5.574	3.875	1.535	1.016	1.778	0.168	0.054
$2_1^+$	1026	5.763	3.739	1.128	1.369	1.868	0.101	0.031
$4_1^+$	1786	5.840	3.738	1.329	1.093	1.925	0.017	0.059
$^{94}\text{Zr}$								
$0_1^+$	0	5.849	3.777	1.171	1.203	3.506	0.449	0.045
$0_2^+$	1603	5.702	3.898	1.274	1.125	3.239	0.720	0.041
$2_1^+$	999	5.864	3.773	1.278	1.086	3.707	0.257	0.036
$4_1^+$	1732	5.896	3.777	1.456	0.871	3.832	0.134	0.034

and use 1.10 ( $-0.10$ ) for the proton (neutron) orbital operator for both interactions. These are rough representations of the nuclear-matter effects calculated<sup>17</sup> and found experimentally.<sup>18</sup> It turns out that this prescription gives essentially the same results as for the free-nucleon operator. However, it was felt necessary to check this point.

Results for  $^{92-94}\text{Zr}$  are summarized in Tables II and III. In Table II we list the predicted mean occupancies of the four protons and three neutron orbits for the levels under discussion. In Table III we list the three  $B(E2)$  values and the  $2_1^+$  magnetic moment for experiment and for both the GI and GJW interactions. The dependence of the results of Table III on the wave functions is very much the same for  $^{92}\text{Zr}$  and  $^{94}\text{Zr}$ . The Gloeckner interaction gives an adequate description of the  $4_1^+ \rightarrow 2_1^+ \rightarrow 0_1^+$  transitions. However, the predicted  $0_2^+ \rightarrow 2_1^+$   $B(E2)$  values are both much too small and the  $2_1^+$  magnetic moments are too negative. It is seen that the GJW interaction does better by a factor  $\geq 5$  for the  $0_2^+ \rightarrow 2_1^+$   $B(E2)$  values and can be made to reproduce these  $0_2^+ \rightarrow 2_1^+$  rates

with only small adjustments in the  $\pi g_{9/2}$  and/or  $\nu s_{1/2}$  SPE. This is also true for the magnetic moments (however, it is difficult to reproduce both data simultaneously by varying only these two SPE). The reason for this improvement has to do with the opening of the proton  $f_{5/2}$  and  $p_{3/2}$  orbits. We find essentially negligible effects from the inclusion of the neutron  $g_{7/2}$  and  $d_{3/2}$  orbits—they become important for Zr isotopes with  $A > 95$ . The  $g_{7/2}$  orbit is particularly unimportant, which is why we omitted it from our model space.

Table II displays a rather state-independent occupancy of the orbits. The most obvious difference between the two nuclei is the increased role of  $\nu s_{1/2}$  as this orbit nears the Fermi surface. We see that inclusion of the proton  $f_{5/2}$  and  $p_{3/2}$  orbits allows considerably increased proton degrees of freedom. The number of protons in the  $p_{1/2}$ - $g_{9/2}$  orbits is increased from 2.0 to  $\sim 2.4$  and this increase is accompanied by  $\sim 0.4$  proton holes in the  $f_{5/2}$ - $p_{3/2}$  orbits. Thus the effective charges necessary to reproduce the  $2_1^+ \rightarrow 0_1^+$   $B(E2)$  are considerably reduced. A not so obvious effect is that the participation of the proton

TABLE III. Comparison of shell-model predictions to experiment for  $^{92}\text{Zr}$  and  $^{94}\text{Zr}$ .  $B(E2)$  values are in W.u.<sup>a</sup> and the magnetic moment,  $\mu(M1)$ , is in nuclear magnetons. The calculation of  $\mu(M1)$  uses the effective operators described in the text.

Transition	Quantity	Experiment	Shell model	
			GI <sup>b</sup>	GJW <sup>c</sup>
$^{92}\text{Zr}$				
$2_1^+ \rightarrow 0_1^+$	$B(E2)$	6.7(5)	5.30	6.40
$0_2^+ \rightarrow 2_1^+$	$B(E2)$	14.3(5)	1.46	8.49
$4_1^+ \rightarrow 2_1^+$	$B(E2)$	4.0(1)	3.41	4.00
$2_1^+ \rightarrow 2_1^+$	$\mu(M1)$	$-0.06(10)$	$-1.18$	$-0.44$
$^{94}\text{Zr}$				
$2_1^+ \rightarrow 0_1^+$	$B(E2)$	5.2(11)	4.58	4.31
$0_2^+ \rightarrow 2_1^+$	$B(E2)$	9.4(4)	0.27	2.78
$4_1^+ \rightarrow 2_1^+$	$B(E2)$	0.88(2)	1.69	1.39
$2_1^+ \rightarrow 2_1^+$	$\mu(M1)$	$-0.52(12)$	$-1.39$	$-0.84$

<sup>a</sup>The ratio between  $B(E2)$  in  $e^2 \text{fm}^{-4}$  and W.u. is 24.672 and 25.390 for  $^{92}\text{Zr}$  and  $^{94}\text{Zr}$ , respectively.

<sup>b</sup> $\delta e_p = 0.765$ ,  $\delta e_n = 1.150$ .

<sup>c</sup> $\delta e_p = \delta e_n \equiv \delta e = 0.60$  was adjusted to reproduce the  $^{92}\text{Zr}$   $4_1^+ \rightarrow 2_1^+$   $B(E2)$ .

$f_{5/2}$ - $p_{3/2}$  orbits brings about a relatively large component of  $(\pi g_{9/2})_{2+}^2$  in the  $2_1^+$  wave function and the contribution of this component to  $\mu(M1)$  approximately cancels that from  $(\nu d_{5/2})_{2+}^2$  thus providing a natural explanation for the small experimental values of  $\mu(M1)$ . Because of this strong cancellation,  $\mu(M1)$  is a strong function of the parameters of the interaction, e.g., the SPE. Thus, it is possible to reproduce the experimental  $\mu(M1)$  with changes in the  $\pi g_{9/2}$  and/or  $\nu s_{1/2}$  SPE of  $\leq 200$  keV.

For the  $0_2^+ \rightarrow 2_1^+$  transition there is no simple explanation for the large change in  $B(E2)$  between the G1 and GJW interactions. In the G1 interaction, the neutron and proton contributions are small, of roughly equal magnitude, and opposite in sign, giving a small  $B(E2)$  value. In the GJW interaction, the neutron contribution is essentially negligible—due partially to destructive contributions from the  $\nu d_{3/2}$  orbit—and the proton contribution for  $e_p = 1.0$  is approximately twice that of the G1 interaction, i.e., without participation of the  $\pi f_{5/2}$ - $p_{3/2}$  orbits.

The experimental  $B(E2)$  values for the  $4_1^+ \rightarrow 2_1^+$  transitions are seen to be rather different in the two nuclei. In both nuclei the calculated neutron and proton contributions to the  $B(E2)$  add coherently just as for the  $2_1^+ \rightarrow 0_1^+$  transitions. Both contributions are less in  $^{94}\text{Zr}$  than in  $^{92}\text{Zr}$ . There does not seem to be a simple reason for this; nevertheless, the calculations predict the observed difference nicely.

The low-lying GJW energy spectra are extremely similar to those reported by Gloeckner if the GJW two-body matrix elements (TBME) are multiplied by 0.86. Presumably this scaling factor represents the increase in model space from the G1 to GJW interactions.

In summary, we have measured the lifetimes of the  $0_2^+$  and  $4_1^+$  levels in  $^{92,94}\text{Zr}$ . Large differences observed in the  $B(E2; 4_1^+ \rightarrow 2_1^+)$  rates and the  $g(2_1^+)$  factors might be construed to imply different structures and in particular a stronger influence of the neutron  $d_{5/2}$  orbit in the low-lying levels in  $^{94}\text{Zr}$  than in  $^{92}\text{Zr}$ , a feature that could have been attributed to a higher purity of the core nucleus of  $^{96}\text{Zr}$ . However, these experimental results are well reproduced in the spherical shell-model calculations which imply strong similarity between  $^{96}\text{Zr}$  and  $^{94}\text{Zr}$  structures. The gross properties are shaped by the neutrons in the  $\nu d_{5/2}$  orbit, while the most obvious difference between the two nuclei is the increased role of  $\nu s_{1/2}$  in  $^{94}\text{Zr}$ . Nevertheless the electromagnetic properties are sensitive to the admixed configurations with a key role played by the proton orbits  $\pi f_{5/2}$  and  $\pi p_{3/2}$  at the Fermi surface.

Stimulating discussions with B. Fogelberg, M. Hass, G. Molnár, and K. Sistemich are gratefully acknowledged. This work was supported in part by the Swedish Natural Science Research Council and the U.S. Department of Energy under Contract No. DE-AC02-76CH00016 with Brookhaven National Laboratory.

<sup>1</sup>H. Mach, G. Molnár, S. Yates, R. L. Gill, A. Aprahamian, and R. A. Meyer, Phys. Rev. C **37**, 254 (1988).

<sup>2</sup>P. Luksch, Nucl. Data Sheets **30**, 573 (1980).

<sup>3</sup>H.-W. Müller, Nucl. Data Sheets **44**, 277 (1985).

<sup>4</sup>S. Raman, C. H. Malarkey, W. T. Milner, C. W. Nestor, and P. H. Stelson, At. Data Nucl. Data Tables **36**, 1 (1987).

<sup>5</sup>D. H. Gloeckner, Nucl. Phys. **A253**, 301 (1975).

<sup>6</sup>M. Hass, C. Broude, Y. Niv, and A. Zemel, Phys. Rev. C **22**, 1065 (1980).

<sup>7</sup>H. Mach, E. K. Warburton, R. L. Gill, R. F. Casten, J. A. Becker, B. A. Brown, and J. A. Winger, Phys. Rev. C **41**, 226 (1990).

<sup>8</sup>H. Mach, R. L. Gill, and M. Moszyński, Nucl. Instrum. Methods **A280**, 49 (1989).

<sup>9</sup>M. Moszyński and H. Mach, Nucl. Instrum. Methods **A277**, 407 (1989).

<sup>10</sup>H. Mach, M. Moszyński, R. L. Gill, F. K. Wohn, J. A. Winger, John C. Hill, G. Molnár, and K. Sistemich, Phys. Lett. B **230**, 21 (1989).

<sup>11</sup>H. Mach *et al.*, Phys. Rev. Lett. **63**, 143 (1989).

<sup>12</sup>R. Julin, J. Kantele, M. Luontama, and A. Passoja, Z. Phys. A **303**, 147 (1981).

<sup>13</sup>X. Ji and B. H. Wildenthal, Phys. Rev. C **37**, 1256 (1988).

<sup>14</sup>B. M. Freedom, E. Newman, and J. C. Hiebert, Phys. Rev. **166**, 1156 (1968).

<sup>15</sup>C. R. Bingham and G. T. Fabian, Phys. Rev. C **7**, 1509 (1973).

<sup>16</sup>B. A. Brown, A. Etchegoyen, W. D. M. Rae, and N. S. Godwin, OXBASH, 1984 (unpublished).

<sup>17</sup>A. Arima, K. Shimizu, W. Bentz, and H. Hyuga, Adv. Nucl. Phys. **18**, 1 (1987).

<sup>18</sup>B. A. Brown and H. B. Wildenthal, Nucl. Phys. **A474**, 290 (1987).